5-2021

Blood Flow Through an Artery in the Presence of a Stenosis

Martin Carrillo
The University of Texas Rio Grande Valley

BLOOD FLOW THROUGH AN ARTERY
IN THE PRESENCE OF A STENOSIS

A Thesis

by

MARTIN CARRILLO

Submitted to the Graduate School of
The University of Texas Rio Grande Valley
In partial fulfillment of the requirements for the degree of

MASTER OF SCIENCE

May 2021

Major Subject: Mathematics

BLOOD FLOW THROUGH AN ARTERY

IN THE PRESENCE OF A STENOSIS

A Thesis
by
MARTIN CARRILLO

COMMITTEE MEMBERS

Dr. Dambaru Bhatta
Chair of Committee

Dr. Andras Balogh
Committee Member

Dr. Paul Bracken
Committee Member

Dr. Zhijun Qiao
Committee Member

May 2021

ABSTRACT

Carrillo, Martin , Blood Flow Through an Artery in the Presence of a Stenosis . Master of Science (MS), May, 2021, 44 pp.,15 tables,25 figures,17 references.

We consider blood flow through an artery in the form of a cylindrical pipe in the presence of a stenosis. Here blood is treated as an incompressible, viscous, and non-Newtonian Bingham plastic fluid. We derive the equation of continuity and the momentum equation which are obtained using mass conservation law and momentum conservation law, respectively. Assuming that the flow is due to the pressure drop and wall shear stress, we derive the expressions for the velocity component in the axial direction and the volumetric flow rate in an artery. Computational results for the axial velocity and flow rate are obtained using MATLAB and presented in tabular and graphical forms to analyze the effects of the slip velocity, pressure difference, yield stress, and stenosis height. Results obtained through our computations indicate that dependent variables (axial velocity and flow rate) increase with the increase in pressure difference and decrease with the increase in yield stress. As stenosis height increases, the dependent variables display a decrease. Both the dependent variables are minimum when the stenosis height is maximum. Increasing the slip velocity enhances the axial velocity and the flow rate.

DEDICATION

This thesis is dedicated to my family and to the memory of my father. They have always supported me in my education and made sure I had everything i needed to be successful.

ACKNOWLEDGMENTS

I express my gratitude towards the thesis committee members especially the committee chair, Dr. Dambaru Bhatta. I thank him for his patience and support as well as for motivating me to never give up. I would like to thank my family for motivating me as well. Lastly, I would like to thank Debbie.

TABLE OF CONTENTS

Page

LIST OF TABLES

Page

LIST OF FIGURES

Page

CHAPTER I

INTRODUCTION

Matter has mainly three forms: solids, liquids, and gases. A solid will not change in shape due to its particle structure. A gas does not have any shape and its particles are scattered which can take up volume in certain environments. A liquid similarly, has particles that can move freely within each other enough to create volume. A fluid is considered compressible if its density fluctuates and is considered incompressible if its density is constant. Most fluids and even gasses are treated as compressible depending on the application. Fluids can also be categorized as either Newtonian or non-Newtonian. A Newtonian fluid is a fluid that follows Newton's law of viscosity. That is, there is a constant linear relationship between the fluid's shear stress and shear rate. A non-Newtonian fluid does not follow Newton's law of viscosity which means that there is non-constant relationship between the fluid's shear stress and shear rate. Some examples of Newtonian fluids include alcohol, water, and gasoline. Fluids such as blood, honey, paint, mayonnaise, ketchup are some examples of non-Newtonian fluid. Chhabra and Richardson [1] presented details on the theory of non-Newtonian fluids. Alderman [2] discussed the classification of non-Newtonian fluids. Blood can be thought of as a liquid due to its mobility. It also contains red blood cells and white blood cells which when analyzed closely, resemble a solid. Together, blood behaves as a liquid and its viscosity can vary depending on the shear stress.

The way blood flows through human body is of great importance for everyone. Understanding how blood flows through our body is a key element in helping us understand how cardiovascular diseases affect us. We can describe blood flow through the heart as the following. The heart contains both blue and red blood vessels that contain deoxygenated blood and

oxygenated blood, respectively. Blood enters the superior vena cava and inferior vena cava and ends up in the right atrium. It then exits through the tricuspid valve and enters the right ventricle. Next, it goes into the pulmonary artery though the pulmonary valve and passes through both the left and right pulmonary arteries. Blood then comes back through the pulmonary veins and then enters the left atrium. It then passes to the left ventricle through the bicuspid valve. Lastly, the blood then leaves through the aortic valve. Our body has arteries that go from our limbs and even to our head. Given this information, if an artery were to become narrow, then that would mean that less blood will be flowing through the heart which can lead major concerns towards someone's health. Figure 1 displays blood flow through the heart [3].

Figure 1: Blood Flow Through Heart

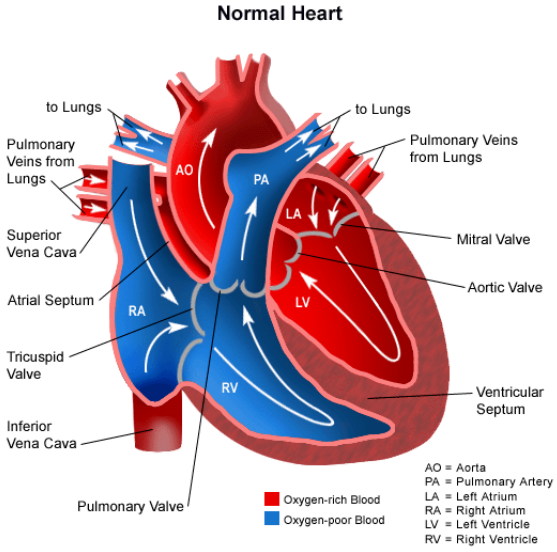

When an artery becomes narrow it is known as stenosis. As an example, we consider coronary artery disease (CAD). CAD is a type of heart disease which affects about 18.2 million adults in the United States [4] . This is a condition in which plaque builds up in the coronary arteries and causes less blood to flow through the heart. This plaque is made up of fat deposits and cholesterol which builds in and on the artery is known as atherosclerosis. As a result, due to the narrowing of the arteries, this can eventually lead to cardiac arrest. Figure 2 compares a normal artery and a stenosed artery [5]. There are several types of heart diseases; each has its

different effects in the body. With heart disease being one of the leading causes of death in the United States [6] , it is of crucial importance to study how blood flows through the artery in different conditions to better understand it.

Figure 2: Normal Artery and Artery Under Stenosis

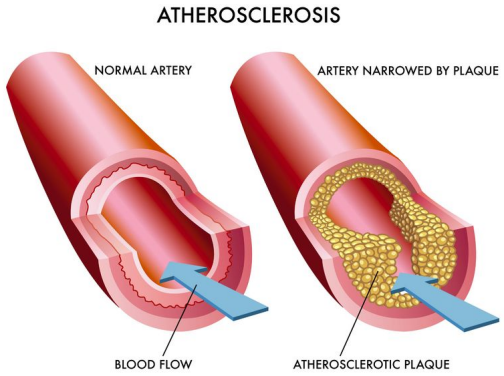

Both Siddiqui [7], and Bhatnagar [8] treated blood as a non-Newtonian fluid and use a Bingham plastic model. Siddiqui, S.U. observed the effect of body acceleration and axial velocity along a constricted artery wall. They found that there is a relationship between viscosity and wall shear stress along with body acceleration. Bhatnagar studies slip velocity and stenosis shape through an artery. Similarly, they found that slip velocity has an effect on the reduction of wall shear stress. Bunonyo [9] studied non-Newtonian blood flow through an artery under the presence of heat in a magnetic field. They discovered that blood velocity is variable depending on how the magnetic field is adjusted. Misra [10] examined the effect of viscoelasticity and wall shear stress of non-Newtonian blood flow in an artery with mild stenosis. Chakravarty [11] observed non-Newtonian blood flow with time-dependent overlapping stenosis. They applied a finite difference approximation to obtain numerical results. Blood is treated as a non-Newtonian Herschel-Bulkley fluid by Sankar [12] and Biswas [13]. Sankar studied blood flow through an asymmetrically stenosed artery by the use of perturbation methods. Mathur [14], Mandal [15], and Ismail [16] all examined non-Newtonian blood flow through the use of a power law model. Mathur found that there is a strong relation with shear stress and pressure drop along with the height of the stenosis. Ismail studied unsteady blood flow through a tapered artery. They obtained

results for different angles for the taper of the stenosed artery. Bhatta and Riahi [17] studied the effect of thermal diffusivity variations due to hydro-thermal convection in a porous media.

In this work, we analyze the blood flow thorough an artery while treating it as a non-Newtonian Bingham plastic fluid. The artery is narrowed down by a stenosis for varying height. To formulate this problem, we first utilize a set of partial differential equations, namely, the equation of continuity and the momentum equation in cylindrical co-ordinates. Also, we assume that the flow is due to the pressure drop in the axial direction and the wall stress only. With these assumptions, we derive the expressions for the axial velocity and volumetric flow rate through the artery. Computational results are obtained using MATLAB and presented in tabular and graphical forms to investigate the effects of the stenosis height, slip velocity, pressure difference, yield stress, and the viscosity.

CHAPTER II

MATHEMATICAL FORMULATION

In this chapter, we derive the equation of continuity, the equation of momentum which we convert into a cylindrical coordinate system. After that, the expressions for axial velocity and volumetric flow rate on a cylindrical pipe are derived.

Equation of Continuity

We consider a fluid occupying a volume V enclosed by a surface S. Let $\overrightarrow{q}\,(\mathbf{r},\,t)$, $\rho\,(\mathbf{r},\,t)$, respectively, denote the velocity and density of the fluid as shown in Figure 3.

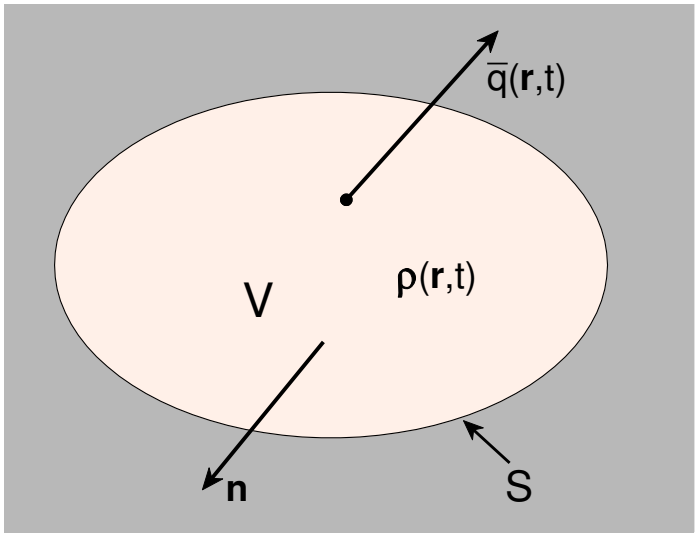

Figure 3: Volume V enclosing the surface S

The mass of fluid enclosed by the surface at any instant is

$$M = \int_V \rho\,(\mathbf{r},\, t)\, dV$$

The rate of change in mass is

$$\frac{dM}{dt} = \frac{d}{dt}\left[\int_V \rho\,(\mathbf{r},\, t)\, dV\right].$$

The total rate at which mass is flowing outwards across the surface is

$$\int_S \rho\,\overrightarrow{q}\cdot\mathbf{n}\, dS.$$

where n represents the unit outward normal to the surface.

In absence of sources/sinks of the fluid the mass of the fluid is conserved, so we obtain

$$\frac{d}{dt}\int_V \rho\, dV = -\int_S \rho\,\overrightarrow{q}\cdot\mathbf{n}\, dS.$$

Carrying out differentiation under the integration (remembering that the volume V is fixed in space) and transforming surface integral to volume integral, we have

$$\int_V \left[\frac{\partial\rho}{\partial t} + div(\rho\,\overrightarrow{q})\right] dV = 0$$

Here V is any arbitrary volume, thus we must have

$$\frac{\partial\rho}{\partial t} + div(\rho\,\overrightarrow{q}) = 0$$
$$\frac{\partial\rho}{\partial t} + \nabla\cdot(\rho\,\overrightarrow{q}) = 0$$

Since

$$\begin{aligned}\nabla\cdot(\rho\,\overrightarrow{q}) &= (\nabla\rho)\cdot\overrightarrow{q} + \rho\,(\nabla\cdot\overrightarrow{q})\\ &= \overrightarrow{q}\cdot\nabla\rho + \rho\nabla\cdot\overrightarrow{q}\end{aligned}$$

The continuity equation becomes

$$\frac{\partial \rho}{\partial t} + \nabla \cdot (\rho \overrightarrow{q}) = 0$$
$$\frac{D\rho}{Dt} + \rho \nabla \cdot \overrightarrow{q} = 0$$

where

$$\frac{D}{Dt} = \frac{\partial}{\partial t} + \overrightarrow{q} \cdot \nabla$$

Continuity Equation for Incompressible Fluid

If the fluid is incompressible, density is treated as constant, Therefore, the continuity equation

$$\frac{\partial \rho}{\partial t} + \nabla \cdot (\rho \overrightarrow{q}) = 0$$

becomes

$$\nabla \cdot \overrightarrow{q} = 0$$

Continuity Equation in Cartesian Co-ordinate System

Suppose

$$\overrightarrow{q} = (u, v, w)$$

where u, v, w represent the x, y, z components of the velocity $\overrightarrow{q}(x, y, z)$.
In 3-D Cartesian co-ordinates, we have

$$\nabla = \left(\frac{\partial}{\partial x}, \frac{\partial}{\partial y}, \frac{\partial}{\partial z}\right)$$

so the continuity equation for incompressible fluid is

$$\frac{\partial u}{\partial x} + \frac{\partial v}{\partial y} + \frac{\partial w}{\partial z} = 0$$

Continuity Equation in Cylindrical Co-ordinate System

Let $v_r,\ v_\theta,\ v_z$ represent the $r,\ \theta,\ z$ components of the velocity $\overrightarrow{q}(r, \theta, z)$.
In Cylindrical co-ordinates, we have the continuity equation for incompressible fluid as

$$\frac{1}{r}\frac{\partial(rv_r)}{\partial r} + \frac{1}{r}\frac{\partial v_\theta}{\partial \theta} + \frac{\partial v_z}{\partial z} = 0$$

Momentum Equation

Here, we consider the elementary control volume V in the form of a cube with sides dx, dy, dz in Cartesian

Figure 4: Control Volume Cube

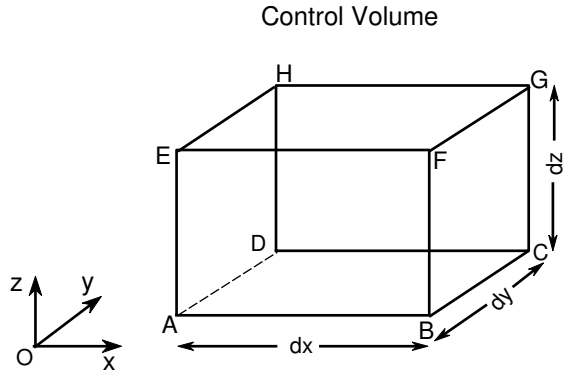

Using mass $\times$ acceleration = force, we can write

$$m\frac{D\overrightarrow{q}}{Dt} = \overrightarrow{F}_p + \overrightarrow{F}_s + \overrightarrow{F}_b$$

where $\overrightarrow{q} = (u, v, w)$ is the velocity vector. $\overrightarrow{F}_p + \overrightarrow{F}_s + \overrightarrow{F}_b$ are respectively , forces due to pressure, stress, body forces, and m is the mass. Also,

$$\frac{D\overrightarrow{q}}{Dt} = \frac{\partial\overrightarrow{q}}{\partial t} + (\overrightarrow{q}\cdot\nabla)\,\overrightarrow{q} = \frac{\partial\overrightarrow{q}}{\partial t} + \overrightarrow{q}\cdot\nabla\,\overrightarrow{q}$$

Figure 5: Various Planes of the Control Volume Cube

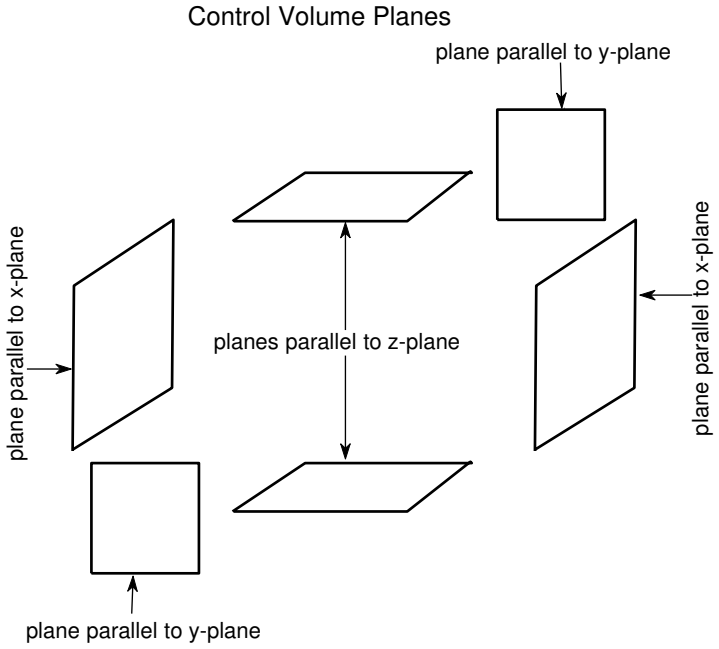

In Figure 5, we see the planes are separated in order to get a better view of their position and direction.

Figure 6: Forces on planes perpendicular to x-axis

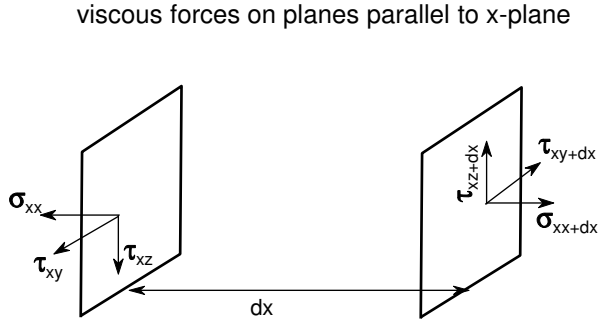

For Figure 6, we see the distance between the planes which is given by dx along with a representation on how the viscous forces act on the $x-$plane.

Figure 7: Forces on planes perpendicular to y-axis

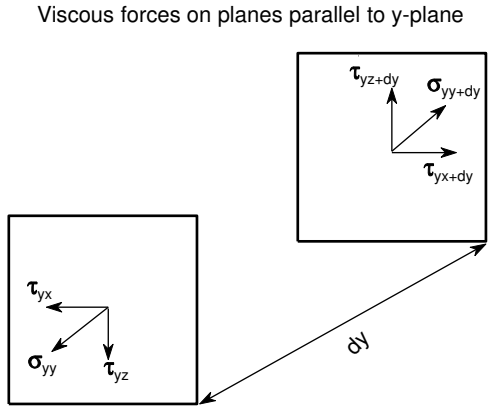

Similarly, for Figure 7 we have the distance dy along with how the viscous forces act on the $y-$plane.

Figure 8: Forces on planes perpendicular to z-axis

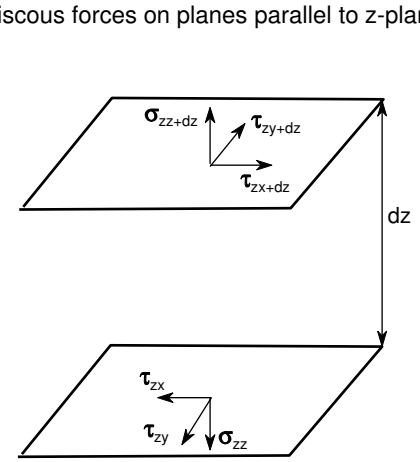

For Figure 8, we have the distance dz along with how the viscous forces act on the $z-$plane.

Now, for the x-direction,

On the planes parallel to x-plane (perpendicular to x-axis)

$$-\sigma_{xx}dydz + \sigma_{xx}dydz + \frac{\partial \sigma_{xx}}{\partial x}dxdydz$$

On the planes parallel to y-plane (perpendicular to y-axis)

$$-\tau_{yx}dxdz + \tau_{yx}dxdz + \frac{\partial \tau_{yx}}{\partial y}dydxdz$$

On the planes parallel to z-plane (perpendicular to z-axis)

$$-\tau_{zx}dxdy + \tau_{zx}dxdy + \frac{\partial \tau_{zx}}{\partial z}dzdxdy$$

Let $V = dx\,dy\,dz$ be volume of the control volume.

Along x-direction,

$$\frac{\partial \sigma_{xx}}{\partial x}V + \frac{\partial \tau_{yx}}{\partial y}V + \frac{\partial \tau_{zx}}{\partial z}V \tag{1}$$

Along y-direction,

$$\frac{\partial \tau_{xy}}{\partial x}V + \frac{\partial \sigma_{yy}}{\partial y}V + \frac{\partial \tau_{zy}}{\partial z}V$$

Along z-direction,

$$\frac{\partial \tau_{xz}}{\partial x}V + \frac{\partial \tau_{yz}}{\partial y}V + \frac{\partial \sigma_{zz}}{\partial z}V$$

Let the body forces be denoted by F_{b_x},F_{b_y},F_{b_z} respectively along x, y and z directions.

Along x-direction,

$$\frac{\partial \sigma_{xx}}{\partial x}V + \frac{\partial \tau_{yx}}{\partial y}V + \frac{\partial \tau_{zx}}{\partial z}V + F_{b_x} = \rho V \frac{Du}{Dt}$$

where ρ is the density of the fluid.

Thus, along x-direction we have

$$\frac{\partial \sigma_{xx}}{\partial x} + \frac{\partial \tau_{yx}}{\partial y} + \frac{\partial \tau_{zx}}{\partial z} + \frac{F_{b_x}}{V} = \rho \frac{Du}{Dt}$$

Similarly, along y-direction

$$\frac{\partial \tau_{xy}}{\partial x} + \frac{\partial \sigma_{yy}}{\partial y} + \frac{\partial \tau_{zy}}{\partial z} + \frac{F_{b_y}}{V} = \rho \frac{Dv}{Dt}$$

and along z-direction

$$\frac{\partial \tau_{xz}}{\partial x} + \frac{\partial \tau_{yz}}{\partial y} + \frac{\partial \sigma_{zz}}{\partial z} + \frac{F_{b_z}}{V} = \rho \frac{Dw}{Dt}$$

Finally, rewriting the external force in x-direction $\frac{F_{b_x}}{V}$ as X, for x-direction we obtain

$$\rho\frac{Du}{Dt} = \frac{\partial\sigma_{xx}}{\partial x} + \frac{\partial\tau_{yx}}{\partial y} + \frac{\partial\tau_{zx}}{\partial z} + X \tag{2}$$

Similarly, along y-direction

$$\rho\frac{Dv}{Dt} = \frac{\partial\tau_{xy}}{\partial x} + \frac{\partial\sigma_{yy}}{\partial y} + \frac{\partial\tau_{zy}}{\partial z} + Y \tag{3}$$

and along z-direction

$$\rho\frac{Dw}{Dt} = \frac{\partial\tau_{xz}}{\partial x} + \frac{\partial\tau_{yz}}{\partial y} + \frac{\partial\sigma_{zz}}{\partial z} + Z \tag{4}$$

From (2), (3) and (4), The momentum equation in vector form is

$$\rho\frac{D\overrightarrow{q}}{Dt} = \nabla\cdot\mathscr{T} + \overrightarrow{F} \tag{5}$$

where $\overrightarrow{F} = (X, Y, Z)$ represents external force (like gravity) and $\mathscr{T}$ is the stress tensor which is given by

$$\mathscr{T} = \begin{bmatrix} \sigma_{xx} & \tau_{xy} & \tau_{xz} \\ \tau_{yx} & \sigma_{yy} & \tau_{yz} \\ \tau_{zx} & \tau_{zy} & \sigma_{zz} \end{bmatrix} \tag{6}$$

Here, since the pressure is perpendicular but opposite in direction, the stress tensor is expressed as

$$\begin{aligned} \mathscr{T} &= \begin{bmatrix} \sigma_{xx} & \tau_{xy} & \tau_{xz} \\ \tau_{yx} & \sigma_{yy} & \tau_{yz} \\ \tau_{zx} & \tau_{zy} & \sigma_{zz} \end{bmatrix} \\ &= -\begin{bmatrix} P & 0 & 0 \\ 0 & P & 0 \\ 0 & 0 & P \end{bmatrix} + \begin{bmatrix} \tau_{xx} & \tau_{xy} & \tau_{xz} \\ \tau_{yx} & \tau_{yy} & \tau_{yz} \\ \tau_{zx} & \tau_{zy} & \tau_{zz} \end{bmatrix} \\ &= -P\mathbf{I} + \mathbf{T} \end{aligned}$$

Given this, the equation (2) becomes

$$\rho\frac{Du}{Dt} = -\frac{\partial P}{\partial x} + \frac{\partial\tau_{xx}}{\partial x} + \frac{\partial\tau_{yx}}{\partial y} + \frac{\partial\tau_{zx}}{\partial z} + X \tag{7}$$

Similarly,

$$\rho\frac{Dv}{Dt} = -\frac{\partial P}{\partial y} + \frac{\partial\tau_{xy}}{\partial x} + \frac{\partial\tau_{yy}}{\partial y} + \frac{\partial\tau_{zy}}{\partial z} + Y \tag{8}$$

and along z-direction

$$\rho\frac{Dw}{Dt} = -\frac{\partial P}{\partial z}+\frac{\partial \tau_{xz}}{\partial x}+\frac{\partial \tau_{yz}}{\partial y}+\frac{\partial \tau_{zz}}{\partial z}+Z \tag{9}$$

Now, the corresponding vector equation is given by

$$\rho\frac{D\overrightarrow{q}}{Dt} = -\nabla P+\nabla\cdot\mathbf{T}+\overrightarrow{F} \tag{10}$$

which is known as the **Momentum Equation.**

For a Newtonian fluid, the stress is proportional to the rate of deformation (the change in velocity in the directions of the stress). Using the Newtonian property, $\tau_{ij}=\mu\left[\frac{\partial u_i}{\partial x_j}+\frac{\partial u_j}{\partial x_i}\right], i,j=1,2,3$, we get

$$\begin{aligned}
&\tau_{xx}=\mu\left[\frac{\partial u}{\partial x}+\frac{\partial u}{\partial x}\right], \quad \tau_{yx}=\mu\left[\frac{\partial v}{\partial x}+\frac{\partial u}{\partial y}\right], \quad \tau_{zx}=\mu\left[\frac{\partial w}{\partial x}+\frac{\partial u}{\partial z}\right]\\
&\tau_{xy}=\mu\left[\frac{\partial u}{\partial y}+\frac{\partial v}{\partial x}\right], \quad \tau_{yy}=\mu\left[\frac{\partial v}{\partial y}+\frac{\partial v}{\partial y}\right], \quad \tau_{zy}=\mu\left[\frac{\partial w}{\partial y}+\frac{\partial v}{\partial z}\right]\\
&\tau_{xz}=\mu\left[\frac{\partial u}{\partial z}+\frac{\partial w}{\partial x}\right], \quad \tau_{yz}=\mu\left[\frac{\partial v}{\partial z}+\frac{\partial w}{\partial y}\right], \quad \tau_{zz}=\mu\left[\frac{\partial w}{\partial z}+\frac{\partial w}{\partial z}\right]
\end{aligned}$$

The proportionality constant μ is known as the viscosity of the fluid. We see that

$$\tau_{xy}=\tau_{yx},\ \tau_{xz}=\tau_{zx},\ \tau_{yz}=\tau_{zy}\,.$$

Due to the symmetry, we have six unknowns. Viscosity defines how easily the fluid flows when subjected to body forces.

For Newtonian fluid

$$\begin{aligned}
\nabla\cdot\mathbf{T} &= \mu\nabla\cdot\begin{bmatrix} 2\frac{\partial u}{\partial x} & \frac{\partial u}{\partial y}+\frac{\partial v}{\partial x} & \frac{\partial u}{\partial z}+\frac{\partial w}{\partial x}\\ \frac{\partial u}{\partial y}+\frac{\partial v}{\partial x} & 2\frac{\partial v}{\partial y} & \frac{\partial v}{\partial z}+\frac{\partial w}{\partial y}\\ \frac{\partial u}{\partial z}+\frac{\partial w}{\partial x} & \frac{\partial v}{\partial z}+\frac{\partial w}{\partial y} & 2\frac{\partial w}{\partial z}\end{bmatrix}\\
&= \mu\begin{bmatrix} \frac{\partial}{\partial x}\left(2\frac{\partial u}{\partial x}\right)+\frac{\partial}{\partial y}\left(\frac{\partial u}{\partial y}+\frac{\partial v}{\partial x}\right)+\frac{\partial}{\partial z}\left(\frac{\partial u}{\partial z}+\frac{\partial w}{\partial x}\right)\\ \frac{\partial}{\partial x}\left(\frac{\partial u}{\partial y}+\frac{\partial v}{\partial x}\right)+\frac{\partial}{\partial y}\left(2\frac{\partial v}{\partial y}\right)+\frac{\partial}{\partial z}\left(\frac{\partial u}{\partial z}+\frac{\partial w}{\partial x}\right)\\ \frac{\partial}{\partial x}\left(\frac{\partial u}{\partial z}+\frac{\partial w}{\partial x}\right)+\frac{\partial}{\partial y}\left(\frac{\partial v}{\partial z}+\frac{\partial w}{\partial y}\right)+\frac{\partial}{\partial z}\left(2\frac{\partial w}{\partial z}\right)\end{bmatrix}'
\end{aligned}$$

Where $'$ is the transpose.

Assuming incompressibility, we have

$$\begin{aligned}\nabla \cdot \mathbf{T} &= \mu \begin{bmatrix} \nabla^2 u + \frac{\partial}{\partial x}\left(\frac{\partial u}{\partial x} + \frac{\partial v}{\partial y} + \frac{\partial w}{\partial z}\right) \\ \nabla^2 v + \frac{\partial}{\partial y}\left(\frac{\partial u}{\partial x} + \frac{\partial v}{\partial y} + \frac{\partial w}{\partial z}\right) \\ \nabla^2 w + \frac{\partial}{\partial z}\left(\frac{\partial u}{\partial x} + \frac{\partial v}{\partial y} + \frac{\partial w}{\partial z}\right) \end{bmatrix}' = \mu\left(\nabla^2 u, \nabla^2 v, \nabla^2 w\right) \\ &= \mu\nabla^2\left(u,\, v,\, w\right) = \mu\nabla^2 \overrightarrow{q}\end{aligned}$$

Finally, this gives us the Navier-Stokes equation which is

$$\rho\frac{D\overrightarrow{q}}{Dt} = -\nabla P + \mu\nabla^2\overrightarrow{q} + \overrightarrow{F}.$$

Conservation of Momentum

Law of mechanics states that mass times acceleration is equal to the sum of forces that act on a volume unit. Total acceleration is composed of the local and the convective acceleration:

$$\frac{D\overrightarrow{q}}{Dt} = \frac{\partial\overrightarrow{q}}{\partial t} + \left(\overrightarrow{q}\cdot\nabla\right)\overrightarrow{q}$$

The momentum equation is

$$\rho\frac{D\overrightarrow{q}}{Dt} = \rho\left[\frac{\partial\overrightarrow{q}}{\partial t} + \left(\overrightarrow{q}\cdot\nabla\right)\overrightarrow{q}\right] = \mathbf{F} + \nabla\cdot\tau$$

where **F** represents external force (like gravity) and σ is the stress tensor.

Laplacian in various Co-ordinate Systems

The Laplacian ∇^2 in 3D Cartesian co-ordinates (x, y, z) becomes

$$\nabla^2 = \frac{\partial^2}{\partial x^2} + \frac{\partial^2}{\partial y^2} + \frac{\partial^2}{\partial z^2}$$

In cylindrical co-ordinates (r, θ, z)

$$\nabla^2 = \frac{\partial^2}{\partial r^2} + \frac{1}{r}\frac{\partial}{\partial r} + \frac{1}{r^2}\frac{\partial^2}{\partial\theta^2} + \frac{\partial^2}{\partial z^2}$$

In cylindrical coordinates

Writing the velocity as $\overrightarrow{\mathbf{q}} = (v_r, v_\theta, v_z)$ and external force as $\mathbf{f} = (f_r, f_\theta, f_z)$, the momentum equations become

$$\rho\left[\frac{\partial v_r}{\partial t} + v_r\frac{\partial v_r}{\partial r} + \frac{v_\theta}{r}\frac{\partial v_r}{\partial \theta} - \frac{v_\theta^2}{r} + v_z\frac{\partial v_r}{\partial z}\right] = -\frac{\partial P}{\partial r} + \frac{1}{r}\frac{\partial}{\partial r}\left(r\tau_{rr}\right) + \frac{1}{r}\frac{\partial \tau_{\theta r}}{\partial \theta} + \frac{\partial \tau_{zr}}{\partial z} - \frac{1}{r}\tau_{\theta\theta} + \rho f_r \tag{11}$$

$$\rho\left[\frac{\partial v_\theta}{\partial t} + v_r\frac{\partial v_\theta}{\partial r} + \frac{v_\theta}{r}\frac{\partial v_\theta}{\partial \theta} + \frac{v_\theta v_r}{r} + v_z\frac{\partial v_\theta}{\partial z}\right] = -\frac{1}{r}\frac{\partial P}{\partial \theta} + \frac{1}{r^2}\frac{\partial}{\partial r}\left(r^2\tau_{r\theta}\right) + \frac{1}{r}\frac{\partial \tau_{\theta\theta}}{\partial \theta} + \frac{\partial \tau_{z\theta}}{\partial z} + \rho f_\theta \tag{12}$$

$$\rho\left[\frac{\partial v_z}{\partial t} + v_r\frac{\partial v_z}{\partial r} + \frac{v_\theta}{r}\frac{\partial v_z}{\partial \theta} + v_z\frac{\partial v_z}{\partial z}\right] = -\frac{\partial P}{\partial z} + \frac{1}{r}\frac{\partial}{\partial r}\left(r\tau_{rz}\right) + \frac{1}{r}\frac{\partial \tau_{\theta z}}{\partial \theta} + \frac{\partial \tau_{zz}}{\partial z} + \rho f_z \tag{13}$$

We consider a steady laminar flow with velocity $\overrightarrow{q}(r, \theta, z)$ with $\overrightarrow{q} = (v_r, v_\theta, v_z)$ in the axial direction of the cylinder. Here v_r denotes the velocity component in radial direction, r; v_θ denotes the velocity component in θ direction, θ; v_z denotes the velocity component in the cylinder axis direction, z. Thus, we have

$$v_z = v(r), \quad v_r = 0, \quad v_\theta = 0, \quad v_z(R) = v_s \tag{14}$$

where v_s represents the slip velocity, i.e, $v_s = v(R)$.

Due to the symmetry of the flow, non-zero contributions from stress tensor come from $\tau_{zr}(r) = \tau_{rz}(r) = \tau$.

For steady state case, using (11)-(13) , we obtain the following

$$\frac{\partial P}{\partial z} - \frac{1}{r}\frac{\partial}{\partial r}(r\,\tau) = 0 \tag{15}$$

$$\frac{\partial P}{\partial r} = 0 \tag{16}$$

τ is finite at $r = 0$.

Since flow in the positive z-direction due to pressure gradient and pressure is decreasing from left to right of the cylinder, we take

$$\frac{\partial P}{\partial z} = K$$

Thus, from (15), we get

$$\frac{\partial}{\partial r}\left[r\,\tau\right] - rK \;=\; 0 \tag{17}$$

On integration, we get

$$r\tau \;=\; \frac{r^2K}{2} + C_1$$

Since τ is finite at $r = 0$, So, $C_1 = 0$. Hence

$$\tau \;=\; \frac{rK}{2} \tag{18}$$

If τ_R represents wall shear stress, we can write

$$\tau_R \;=\; \frac{R(z)K}{2}$$

Non-Newtonian Bingham Fluid

For Bingham Fluid, we have

$$\frac{dv}{dr} \;=\; \frac{\tau_0 - \tau}{\mu} \qquad for\;\; \tau \geq \tau_0 \tag{19}$$

$$\frac{dv}{dr} \;=\; 0 \qquad for\;\; \tau < \tau_0 \tag{20}$$

where τ_0 represents the yield stress and μ is the viscosity. From (19) and (18), we obtain

$$\frac{dv}{dr} \;=\; \frac{1}{\mu}\left\{\tau_0 - \tau\right\} = \frac{1}{\mu}\left\{\tau_0 - \frac{rK}{2}\right\}$$

Hence, integrating

$$v(r) \;=\; \frac{1}{\mu}\left\{r\tau_0 - \frac{r^2K}{4}\right\} + C_2$$

Using slip velocity, v_s as $v = v_s$ at $r = R(z)$,

$$C_2 \;=\; v_s - \frac{1}{\mu}\left\{R\tau_0 - \frac{R^2K}{4}\right\}$$

So, finally, we have

$$\begin{aligned} v(r) \;&=\; \frac{1}{\mu}\left\{r\tau_0 - \frac{r^2K}{4}\right\} + v_s - \frac{1}{\mu}\left\{R\tau_0 - \frac{R^2K}{4}\right\} \\ &=\; v_s + \frac{K}{4\mu}\left(R^2 - r^2\right) - \frac{\tau_0}{\mu}\left(R - r\right) \qquad for \quad r_b \leq r \leq R \end{aligned}$$

When $r = r_b$, $\tau_0 = \frac{r_b K}{2}$, it is found that

$$\begin{aligned} v(r) &= v_s + \frac{K}{4\mu}\left(R^2 - r_b^2\right) - \frac{\tau_0}{\mu}\left(R - r_b\right) \\ &= v_s + \frac{K}{4\mu}\left\{\left(R^2 - r_b^2\right) - \frac{4\tau_0}{K}\left(R - r_b\right)\right\} \\ &= v_s + \frac{K}{4\mu}\left\{\left(R^2 - r_b^2\right) - 2r_b\left(R - r_b\right)\right\} \\ &= v_s + \frac{K}{4\mu}\left\{R^2 - 2r_b R + r_b^2\right\} \\ &= v_s + \frac{K}{4\mu}\left(R - r_b\right)^2 \\ &= v_s + \frac{K}{4\mu}\left(R - \frac{2\tau_0}{K}\right)^2 \qquad for \quad 0 \le r \le r_b \end{aligned}$$

Here, r_b denotes the radius of the solid central portion of the artery.

Computation of Volumetric flow rate

The volumetric flow rate Q through the annulus which is formed by the two concentric circles of radius r and $(r + dr)$ is given by

$$dQ = 2\pi r v_z(r) dr$$

Integrating with respect to r from 0 to $R(z)$, we obtain

$$Q = \int_0^{R(z)} 2\pi r v_z dr$$

This can be written as

$$Q = \int_0^R 2\pi r v_z dr = \int_0^{r_b} 2\pi r v_b dr + \int_{r_b}^R 2\pi r v_z dr$$

i.e.,

$$Q = Q_1 + Q_2$$

where

$$\begin{aligned} Q_1 &= \int_0^{r_b} 2\pi r v_b dr \\ &= 2\pi \int_0^{R_b} r \frac{KR^2}{4\mu}\left(1 - \frac{r_b}{R}\right)^2 dr \\ &= \frac{\pi K R^2}{4\mu} r_b^2 \left(1 - \frac{r_b}{R}\right)^2 \end{aligned}$$

and

$$\begin{aligned}
Q_2 =& 2\pi \int_{r_b}^{R} r \left\{ \frac{KR^2}{4\mu} \left(1 - \frac{r^2}{R^2}\right) - \frac{\tau_0 R}{\mu} \left(1 - \frac{r}{R}\right) \right\} dr \\
=& 2\pi \cdot \frac{KR^2}{4\mu} \left[\frac{r^2}{2} - \frac{r^4}{4R^2} \right]_{r_b}^{R} - 2\pi \cdot \frac{\tau_0 R}{\mu} \left[\frac{r^2}{2} - \frac{r^3}{3r} \right]_{r_b}^{R} \\
=& \frac{\pi K R^2}{4\mu} \left\{ \left(R^2 - \frac{R^4}{2R^2} \right) - \left(r_b^2 - \frac{r_b^4}{2R^2} \right) \right\} \\
& - \frac{\pi \tau_0 R}{\mu} \left\{ \left(R^2 - \frac{2R^2}{3} \right) - \left(r_b^2 - \frac{2r_b^3}{3R} \right) \right\} \\
=& \frac{\pi K R^2}{4\mu} \left\{ \frac{R^2}{2} - r_b^2 \left(1 - \frac{r_b^2}{2R^2}\right) \right\} \\
& - \frac{\pi \tau_0 R}{\mu} \left\{ \frac{R^2}{3} - r_b^2 \left(1 - \frac{2r_b}{3R}\right) \right\}.
\end{aligned}$$

Taking $\alpha = \frac{r_b}{R}$, we have

$$Q_1 = \frac{\pi K R^4}{4\mu} \alpha^2 (1 - \alpha)^2$$

and

$$Q_2 = \frac{\pi K R^4}{4\mu} \left\{ \frac{1}{2} - \alpha^2 \left(1 - \frac{1}{2}\alpha^2\right) \right\} - \frac{\pi \tau_0 R^3}{\mu} \left\{ \frac{1}{3} - \alpha \left(1 - \frac{2}{3}\alpha\right) \right\}$$

Further simplification of Q_2 gives us the following. Let $\tau = \frac{rK}{2}$, and $\tau_0 = \frac{r_b K}{2}$,

$$\begin{aligned}
Q_2 =& \frac{\pi K R^4}{8\mu} \left[1 - 2\alpha^2 + \alpha^4 - \frac{\tau_0}{RK} \left(\frac{8}{3} - 8\alpha^2 + \frac{16\alpha^3}{3} \right) \right] \\
=& \frac{\pi K R^4}{8\mu} \left[1 - 2\alpha^2 + \alpha^4 - \frac{\alpha}{2} \left(\frac{8}{3} - 8\alpha^2 + \frac{16\alpha^3}{3} \right) \right] \\
=& \frac{\pi K R^4}{8\mu} \left[1 - 2\alpha^2 + \alpha^4 - \frac{4\alpha}{3} + 4\alpha^3 - \frac{8\alpha^4}{3} \right].
\end{aligned}$$

Now, we find the sum of Q_1 and Q_2 to find Q. So,

$$
\begin{aligned}
Q =& Q_1 + Q_2 \\
=& \frac{\pi K R^4}{8\mu} \left[2\alpha^2 (1-\alpha)^2 + 1 - 2\alpha^2 + \alpha^4 - \frac{4\alpha}{3} + 4\alpha^3 - \frac{8\alpha^4}{3} \right] \\
=& \frac{\pi K R^4}{8\mu} \left[2\alpha^2 - 4\alpha^3 + 2\alpha^4 + 1 - 2\alpha^2 + \alpha^4 - \frac{4\alpha}{3} + 4\alpha^3 - \frac{8\alpha^4}{3} \right] \\
=& \frac{\pi K R^4}{8\mu} \left[2\alpha^4 + 1 + \alpha^4 - \frac{4\alpha}{3} - \frac{8\alpha^4}{3} \right] \\
=& \frac{\pi K R^4}{8\mu} \left[1 - \frac{4\alpha}{3} + \frac{\alpha^4}{3} \right]
\end{aligned}
$$

To incorporate the slip velocity, v_s to the above result, we add $\pi R^2 v_s$ term. Hence, the flow rate Q becomes

$$
\begin{aligned}
Q &= \pi R^2 v_s + \frac{\pi K R^4}{8\mu} \left[1 - \frac{4\alpha}{3} + \frac{\alpha^4}{3} \right] \\
&= \pi R^2 \left[v_s + \frac{K R^2}{8\mu} \left\{ 1 - \frac{4\alpha}{3} + \frac{\alpha^4}{3} \right\} \right]
\end{aligned}
$$

CHAPTER III

ARTERY WITH STENOSIS

We set up the stenosed artery by constructing a cylindrical pipe along with a symmetrically stenosed region. We derive the equation that represents the radius from the center of the artery to the maximum height of the stenosis.

Figure 9: Geometry of Artery with a Stenosis

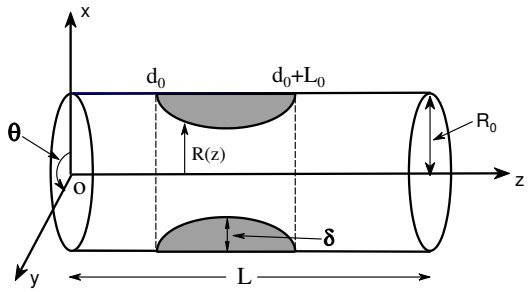

Here, we are given an artery on a cylindrical coordinate system where d_0 is the distance to the start of the stenosis. L_0 is the length of the stenosis. R_0 represent the radius of the non-stenosed artery and $R(z)$ represents the radius of the artery. Lastly, δ represents the maximum height of the stenosis.

We consider the form of the stenosis to be a quadratic function.

So,

$$R(z) = \begin{cases} R_0[A(z-d_0)(z-d_0-L_0)+1] & \text{for } d_0 \le z \le d+L_0, \quad A>0, \\ R_0 & \text{otherwise.} \end{cases}$$

with

$$z = d_0 \implies R(z) = R_0$$

and

$$z = L_0 + d_0 \implies R(z) = R_0.$$

Here, we take A to be strictly positive. Rewriting $R(z)$ above, we have

$$R(z) = R_0 \left[A\{(z - d_0)^2 - L_0(z - d_0)\} + 1 \right]$$

Taking its first and second derivative gives us

$$\frac{d}{dz} R(z) = R_0[A\{2(z - d_0) - L_0\}]$$

$$\frac{d^2}{dz^2} R(z) = 2A$$

which is positive as $A > 0$, implying there is a minimum. To find the location of the minimum, we set $R'(z) = 0$. So,

$$R'(z) = R_0[A\{2(z - d_0) - L_0\}] = 0$$

$$\implies A\{2(z - d_0) - L_0\} = 0$$

$$\implies 2(z - d_0) - L_0 = 0$$

which gives

$$z = d_0 + \frac{L_0}{2}$$

Now, from the figure above, we see that our midpoint of the stenosis would be given by

$$\frac{d_0 + d_0 + L_0}{2}$$

$$= \frac{2d_0 + L_0}{2}$$

$$= d_0 + \frac{L_0}{2}$$

Thus, the location of the minimum is at

$$z = d_0 + \frac{L_0}{2}$$

So, the minimum is given by

$$R_{min} = R_0 \left[A \left\{ \left(\frac{L_0}{2} \right)^2 - \frac{L_0^2}{2} \right\} + 1 \right]$$

$$= R_0 \left(1 - \frac{AL_0^2}{4} \right).$$

We assume the maximum height of the stenosis is given by δ. So,

$$\begin{aligned} \delta &= R_0 - R_{\text{min}} \\ &= R_0 - R_0 \left(1 - \frac{AL_0^2}{4} \right) \\ &= \frac{AR_0 L_0^2}{4} \end{aligned}$$

Therefore,

$$A = \frac{4\delta}{R_0 L_0^2}.$$

Finally, the stenosis shape function, $R(z)$, becomes

$$R(z) = \begin{cases} R_0 \left[\frac{4\delta}{R_0 L_0^2} \left\{ (z - d_0)^2 - L_0 (z - d_0) \right\} + 1 \right] & \text{for } d_0 \leq z \leq d + L_0, \\ R_0 & \text{otherwise.} \end{cases}$$

CHAPTER IV

RESULTS AND DISCUSSIONS

We present computational results for the axial velocity $v_z(r)$ and the flow rate Q through the artery. For all our computational work, MATLAB has been used. We take $L = 3$, the length of the stenosis is $d_0 = 1$and the start of the stenosis is at $L_0 = 1$. Also we consider the radius of the artery without stenosis to be 1. i.e. . $R_0 = 1$. This geometry is depicted in Figure 10.

Figure 10: Artery segment with $L = 3$, $d_0 = 1$, and $L_0 = 1$

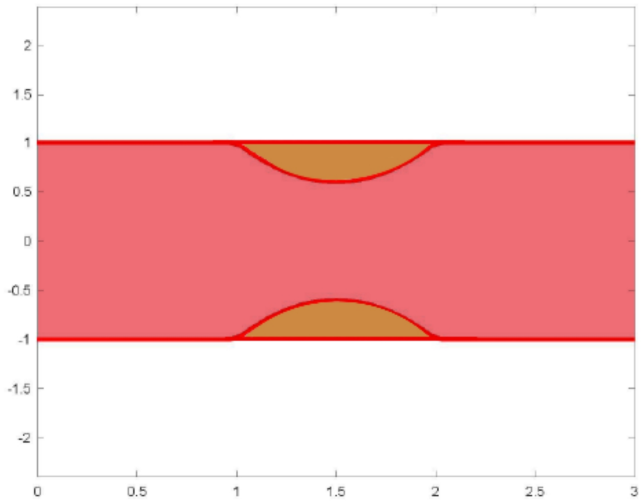

Table 1 and Table 2 provide the axial velocity for different z values. We use the parameter $\tau_0 = 0.2$, $\mu = 0.4$, $K = 8$, $\delta = 0.3$, and $v_s = 0.1$ for our computations. We see that the values of the axial velocity are higher at $z = 0.8$, but are lower at $z = 1.5$. This indicates that the axial velocity is decreasing as we approach the max stenosis height at $z = 1.5$.

Table 1: Axial Velocity Data for $z = 0.8, 1.1$

$z = 0.8$			$z = 1.1$		
r	$\frac{r}{R}$	v	r	$\frac{r}{R}$	v
0.00	0.00	4.6125	0.00	0.00	3.6448
0.07	0.07	4.6102	0.06	0.07	3.6439
0.14	0.14	4.5694	0.13	0.14	3.6148
0.21	0.21	4.4776	0.19	0.21	3.5452
0.29	0.29	4.3347	0.25	0.29	3.4350
0.36	0.36	4.1408	0.32	0.36	3.2842
0.43	0.43	3.8959	0.38	0.43	3.0928
0.50	0.50	3.6000	0.45	0.50	2.8607
0.57	0.57	3.2531	0.51	0.57	2.5881
0.64	0.64	2.8551	0.57	0.64	2.2749
0.71	0.71	2.4061	0.64	0.71	1.9211
0.79	0.79	1.9061	0.70	0.79	1.5267
0.86	0.86	1.3551	0.76	0.86	1.0918
0.93	0.93	0.7531	0.83	0.93	0.6162
1.00	1.00	0.1000	0.89	1.00	0.1000

Table 2: Axial Velocity Data for $z = 1.2, 1.5$

$z = 1.2$			$z = 1.5$		
r	$\frac{r}{R}$	v	r	$\frac{r}{R}$	v
0.00	0.00	2.9728	0.00	0.00	2.2125
0.06	0.07	2.9725	0.05	0.07	2.2125
0.12	0.14	2.9514	0.10	0.14	2.2000
0.17	0.21	2.8970	0.15	0.21	2.1625
0.23	0.29	2.8093	0.20	0.29	2.1000
0.29	0.36	2.6882	0.25	0.36	2.0125
0.35	0.43	2.5339	0.30	0.43	1.9000
0.40	0.50	2.3462	0.35	0.50	1.7625
0.46	0.57	2.1253	0.40	0.57	1.6000
0.52	0.64	1.8710	0.45	0.64	1.4125
0.58	0.71	1.5834	0.50	0.71	1.2000
0.63	0.79	1.2625	0.55	0.79	0.9625
0.69	0.86	0.9083	0.60	0.86	0.7000
0.75	0.93	0.5208	0.65	0.93	0.4125
0.81	1.00	0.1000	0.70	1.00	0.1000

In Figure 11, we present the axial velocity for different z values. We use the parameters $\mu = 0.4$,$\tau_0 = 0.2$, $K = 8$, $\delta = 0.3$,and $v_s = 0.1$. The velocity is the highest when $z = 0.8$ and

is lowest when $z = 1.5$. Thus, as z approaches the maximum stenosis height the axial velocity is decreasing and it becomes minimum at $z = 1.5$.

Figure 11: Axial Velocity for z

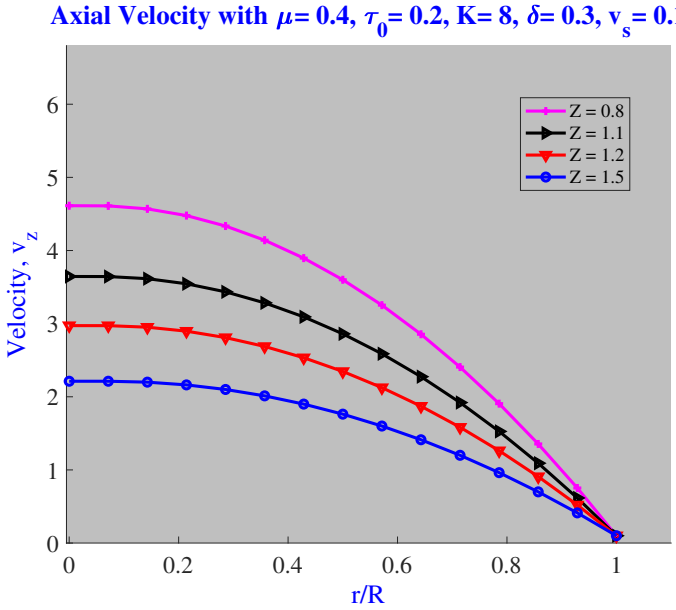

Table 3 and Table 4 provide the effect of slip velocity for the parameters $\mu = 0.4$,$\tau_0 = 0.2$, $\delta = 0.3$, $K = 8$, and $z = 0.8$. for $v_s = 0, 0.4, 0.7, 1$. We see that our axial velocity v is increasing as the slip velocity is increasing.

Table 3: Axial Velocity Data for $v_s = 0.0, 0.4$ with $z = 0.8$

$v_s = 0.0$			$v_s = 0.4$		
r	$\frac{r}{R}$	v	r	$\frac{r}{R}$	v
0.00	0.00	2.1125	0.00	0.00	2.5125
0.05	0.07	2.1125	0.05	0.07	2.5125
0.10	0.14	2.1000	0.10	0.14	2.5000
0.15	0.21	2.0625	0.15	0.21	2.4625
0.20	0.29	2.0000	0.20	0.29	2.4000
0.25	0.36	1.9125	0.25	0.36	2.3125
0.30	0.43	1.8000	0.30	0.43	2.2000
0.35	0.50	1.6625	0.35	0.50	2.0625
0.40	0.57	1.5000	0.40	0.57	1.9000
0.45	0.64	1.3125	0.45	0.64	1.7125
0.50	0.71	1.1000	0.50	0.71	1.5000
0.55	0.79	0.8625	0.55	0.79	1.2625
0.60	0.86	0.6000	0.60	0.86	1.0000
0.65	0.93	0.3125	0.65	0.93	0.7125
0.70	1.00	0.0000	0.70	1.00	0.4000

Table 4: Axial Velocity Data for $v_s = 0.7, 1.0$ with $z = 0.8$

$v_s = 0.7$			$v_s = 1.0$		
r	$\frac{r}{R}$	v	r	$\frac{r}{R}$	v
0.00	0.00	2.8125	0.00	0.00	3.1125
0.05	0.07	2.8125	0.05	0.07	3.1125
0.10	0.14	2.8000	0.10	0.14	3.1000
0.15	0.21	2.7625	0.15	0.21	3.0625
0.20	0.29	2.7000	0.20	0.29	3.0000
0.25	0.36	2.6125	0.25	0.36	2.9125
0.30	0.43	2.5000	0.30	0.43	2.8000
0.35	0.50	2.3625	0.35	0.50	2.6625
0.40	0.57	2.2000	0.40	0.57	2.5000
0.45	0.64	2.0125	0.45	0.64	2.3125
0.50	0.71	1.8000	0.50	0.71	2.1000
0.55	0.79	1.5625	0.55	0.79	1.8625
0.60	0.86	1.3000	0.60	0.86	1.6000
0.65	0.93	1.0125	0.65	0.93	1.3125
0.70	1.00	0.7000	0.70	1.00	1.0000

Figure 12 displays the axial velocity for different v_s values. We consider the parameters $\mu = 0.4$,$\tau_0 = 0.2$, $K = 8$, $\delta = 0.3$,and $z = 0.8$. We see that the axial velocity is increasing when from $v_s = 0$ to $v_s = 1$. Hence, as the axial velocity is increasing, the slip velocity is also increasing.

Figure 12: Axial Velocity for v_s at $z = 0.8$

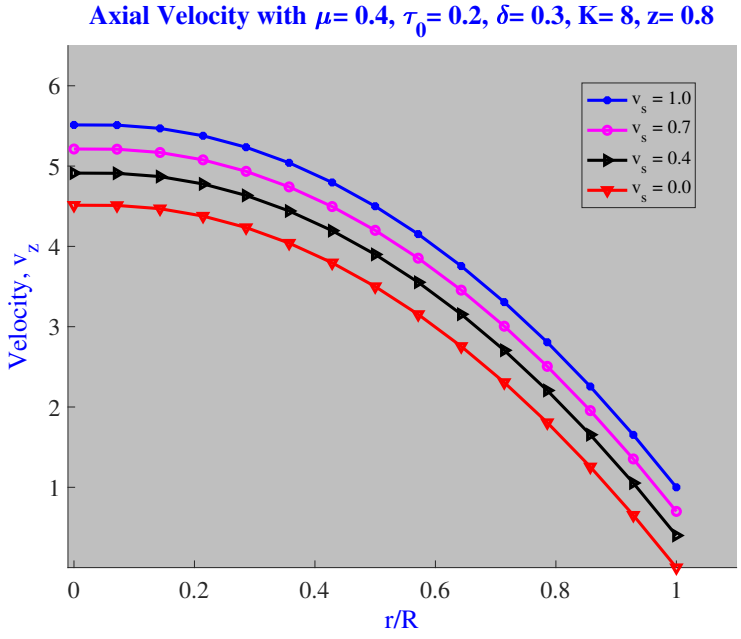

In Figure 13, we have the axial velocity for different v_s values. We consider the parameters

$\mu = 0.4$,$\tau_0 = 0.2$, $K = 8$, $\delta = 0.3$,and $z = 1.5$. We see that the overall velocity has decreased compared to when $z = 0.8$. Similar to when $z = 0.8$, the axial velocity is increasing as the slip velocity is increasing.

Figure 13: Axial Velocity for v_s at $z = 1.5$

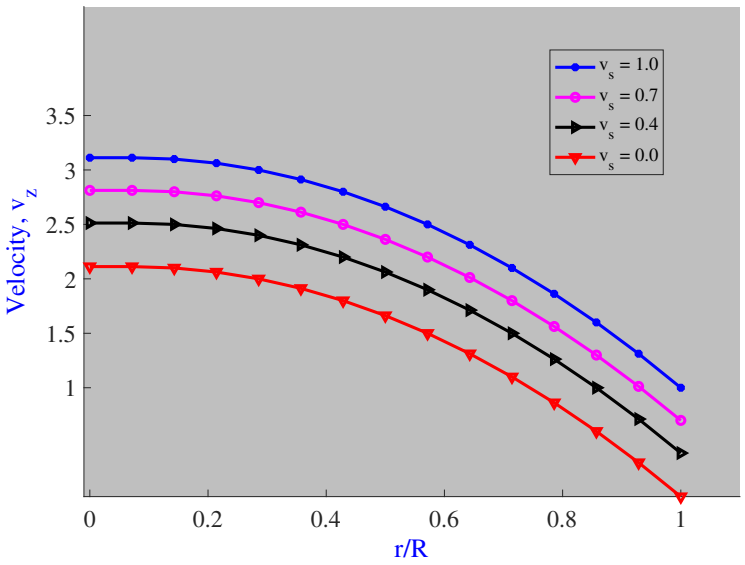

In Figure 14, we present the axial velocity for different τ_0 values. We use the parameters $\mu = 0.4$, $v_s = 0.1$, $K = 8$, $\delta = 0.3$,and $z = 0.8$. The velocity here is at its highest when the yield stress is at $\tau_0 = 0.1$. Therefore, as the yield stress is increasing, the axial velocity is decreasing.

Figure 14: Axial Velocity for τ_0 at $z = 0.8$

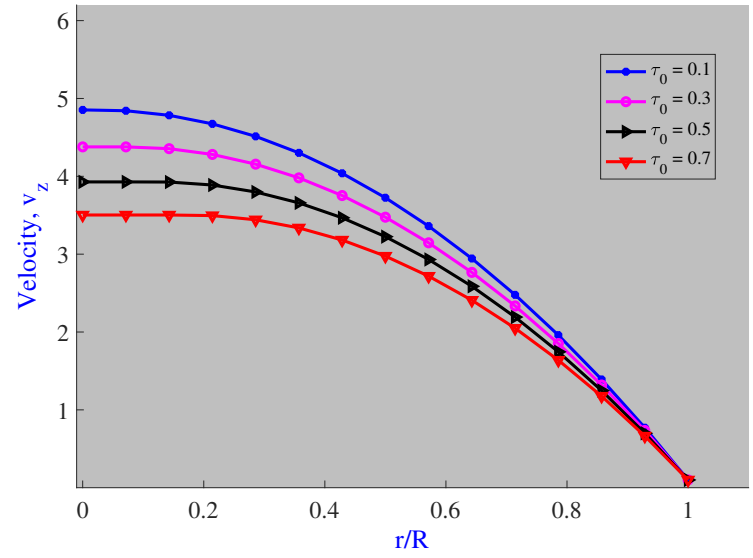

In Table 5 and Table 6, we present the yield stress for parameters $\mu = 0.4$, $v_s = 0.1$, $K = 8$, $\delta = 0.3$, and $z = 1.5$. We notice that as τ_0 increases from $\tau_0 = 0.1$ to $\tau = 0.7$, the v values are decreasing. Thus, as the yield stress is increasing, the axial velocity is decreasing.

Table 5: Axial Velocity Data for $\tau_0 = 0.1, 0.3$ with $z = 1.5$

$\tau_0 = 0.1$			$\tau_0 = 0.3$		
r	$\frac{r}{R}$	v	r	$\frac{r}{R}$	v
0.00	0.00	2.3781	0.00	0.00	2.0531
0.05	0.07	2.3750	0.05	0.07	2.0531
0.10	0.14	2.3500	0.10	0.14	2.0500
0.15	0.21	2.3000	0.15	0.21	2.0250
0.20	0.29	2.2250	0.20	0.29	1.9750
0.25	0.36	2.1250	0.25	0.36	1.9000
0.30	0.43	2.0000	0.30	0.43	1.8000
0.35	0.50	1.8500	0.35	0.50	1.6750
0.40	0.57	1.6750	0.40	0.57	1.5250
0.45	0.64	1.4750	0.45	0.64	1.3500
0.50	0.71	1.2500	0.50	0.71	1.1500
0.55	0.79	1.0000	0.55	0.79	0.9250
0.60	0.86	0.7250	0.60	0.86	0.6750
0.65	0.93	0.4250	0.65	0.93	0.4000
0.70	1.00	0.1000	0.70	1.00	0.1000

Table 6: Axial Velocity Data for $\tau_0 = 0.5, 0.7$ with $z = 1.5$

$\tau_0 = 0.5$			$\tau_0 = 0.7$		
r	$\frac{r}{R}$	v	r	$\frac{r}{R}$	v
0.00	0.00	1.7531	0.00	0.00	1.4781
0.05	0.07	1.7531	0.05	0.07	1.4781
0.10	0.14	1.7531	0.10	0.14	1.4781
0.15	0.21	1.7500	0.15	0.21	1.4781
0.20	0.29	1.7250	0.20	0.29	1.4750
0.25	0.36	1.6750	0.25	0.36	1.4500
0.30	0.43	1.6000	0.30	0.43	1.4000
0.35	0.50	1.5000	0.35	0.50	1.3250
0.40	0.57	1.3750	0.40	0.57	1.2250
0.45	0.64	1.2250	0.45	0.64	1.1000
0.50	0.71	1.0500	0.50	0.71	0.9500
0.55	0.79	0.8500	0.55	0.79	0.7750
0.60	0.86	0.6250	0.60	0.86	0.5750
0.65	0.93	0.3750	0.65	0.93	0.3500
0.70	1.00	0.1000	0.70	1.00	0.1000

In Figure 15, we consider the axial velocity for different τ_0. We consider the parameters $\mu = 0.4$,$\tau_0 = 0.2$, $K = 8$, $\delta = 0.3$,and $z = 1.5$. Here, we see that the overall velocity values are lower compared to $z = 0.8$. Similarly, as the yield stress is increasing, the axial velocity is decreasing.

Figure 15: Axial Velocity for τ_0 at $z = 1.5$

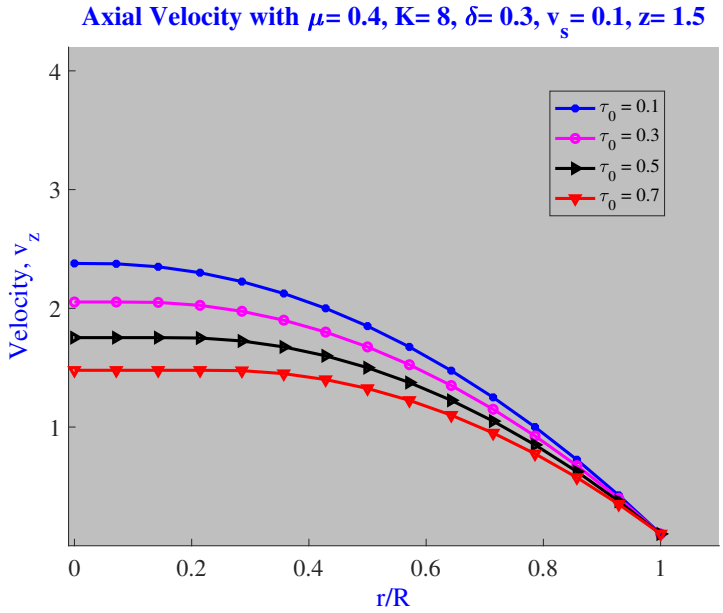

For Table 7 and Table 8, we have the axial velocity for different μ with parameters $\tau_0 = 0.2$, $K = 8$, $\delta = 0.3$, $v_s = 0.1$, and $z = 0.8$. Here, axial velocity is at its highest when $\mu = 0.3$ and at its lowest when $\mu = 0.6$. Therefore, as the viscosity is increasing, the axial velocity is decreasing.

Table 7: Axial Velocity Data for $\mu = 0.3, 0.4$ with $z = 0.8$

$\mu = 0.3$			$\mu = 0.4$		
r	$\frac{r}{R}$	v	r	$\frac{r}{R}$	v
0.00	0.00	6.1167	0.00	0.00	4.6125
0.07	0.07	6.1136	0.07	0.07	4.6102
0.14	0.14	6.0592	0.14	0.14	4.5694
0.21	0.21	5.9367	0.21	0.21	4.4776
0.29	0.29	5.7463	0.29	0.29	4.3347
0.36	0.36	5.4878	0.36	0.36	4.1408
0.43	0.43	5.1612	0.43	0.43	3.8959
0.50	0.50	4.7667	0.50	0.50	3.6000
0.57	0.57	4.3041	0.57	0.57	3.2531
0.64	0.64	3.7735	0.64	0.64	2.8551
0.71	0.71	3.1748	0.71	0.71	2.4061
0.79	0.79	2.5082	0.79	0.79	1.9061
0.86	0.86	1.7735	0.86	0.86	1.3551
0.93	0.93	0.9707	0.93	0.93	0.7531
1.00	1.00	0.1000	1.00	1.00	0.1000

Table 8: Axial Velocity Data for $\mu = 0.5, 0.6$ with $z = 0.8$

$\mu = 0.5$			$\mu = 0.6$		
r	$\frac{r}{R}$	v	r	$\frac{r}{R}$	v
0.00	0.00	3.7100	0.00	0.00	3.1083
0.07	0.07	3.7082	0.07	0.07	3.1068
0.14	0.14	3.6755	0.14	0.14	3.0796
0.21	0.21	3.6020	0.21	0.21	3.0184
0.29	0.29	3.4878	0.29	0.29	2.9231
0.36	0.36	3.3327	0.36	0.36	2.7939
0.43	0.43	3.1367	0.43	0.43	2.6306
0.50	0.50	2.9000	0.50	0.50	2.4333
0.57	0.57	2.6224	0.57	0.57	2.2020
0.64	0.64	2.3041	0.64	0.64	1.9367
0.71	0.71	1.9449	0.71	0.71	1.6374
0.79	0.79	1.5449	0.79	0.79	1.3041
0.86	0.86	1.1041	0.86	0.86	0.9367
0.93	0.93	0.6224	0.93	0.93	0.5354
1.00	1.00	0.1000	1.00	1.00	0.1000

For Figure 16, we have the axial velocity for μ. The parameters used are $\tau_0 = 0.2$, $K = 8$, $\delta = 0.3$, $v_s = 0.1$, and $z = 0.8$. Here, the axial velocity is at its highest when $\mu = 0.3$. Thus, as the viscosity μ is increasing, the axial velocity is decreasing.

Figure 16: Axial Velocity for μ at $z = 0.8$

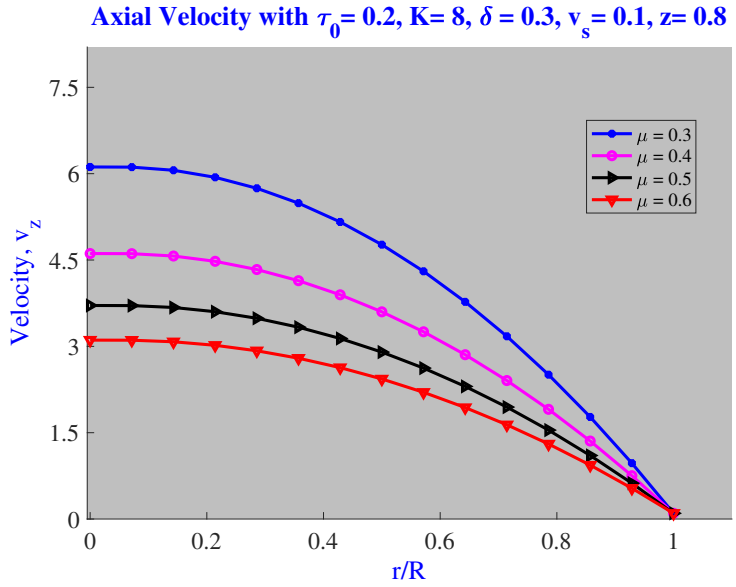

For Figure 17, we have the axial velocity for μ. The parameters used are $\tau_0 = 0.2$,$K = 8$,$\delta = 0.3$,$v_s = 0.1$, and $z = 1.5$. Here, we see that the velocities are lower than when $z = 0.8$. Similarly, the viscosity μ is increasing as the axial velocity is decreasing.

Figure 17: Axial Velocity for μ at $z = 1.5$

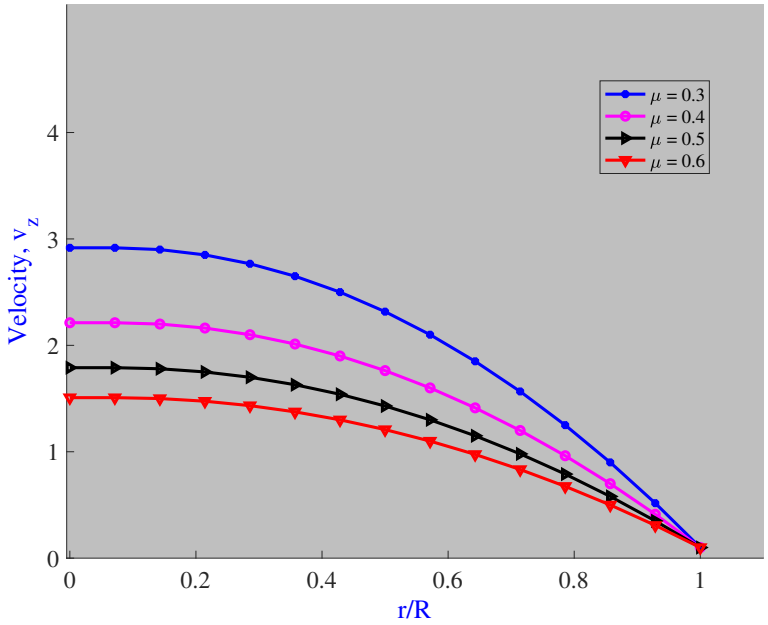

Figure 18 presents the axial velocity for various pressure difference K. We use the parameters $\mu = 0.4$,$\tau_0 = 0.2$,$\delta = 0.3$,$v_s = 0.1$, and $z = 0.8$. We see that when the pressure difference is

at $K = 12$, we have the highest axial velocity. Hence, as the pressure difference is increasing, the axial velocity is increasing.

Figure 18: Axial Velocity for K at $z = 0.8$

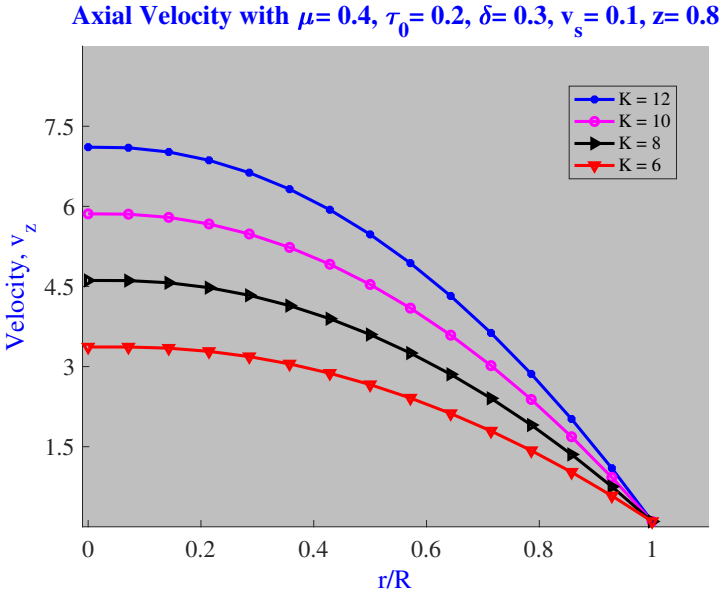

For Table 9 and Table 10, we have the axial velocity for the pressure difference K. We use the parameters $\mu = 0.4$,$\tau_0 = 0.2$,$\delta = 0.3$,$v_s = 0.1$, and $z = 1.5$. We notice that the v values are increasing as K is increasing. Therefore, we can say that pressure difference is increasing as the axial velocity is increasing.

Table 9: Axial Velocity Data for $K = 6, 8$ with $z = 1.5$

$K = 6$			$K = 8$		
r	$\frac{r}{R}$	v	r	$\frac{r}{R}$	v
0.00	0.00	1.6042	0.00	0.00	2.2125
0.05	0.07	1.6042	0.05	0.07	2.2125
0.10	0.14	1.6000	0.10	0.14	2.2000
0.15	0.21	1.5781	0.15	0.21	2.1625
0.20	0.29	1.5375	0.20	0.29	2.1000
0.25	0.36	1.4781	0.25	0.36	2.0125
0.30	0.43	1.4000	0.30	0.43	1.9000
0.35	0.50	1.3031	0.35	0.50	1.7625
0.40	0.57	1.1875	0.40	0.57	1.6000
0.45	0.64	1.0531	0.45	0.64	1.4125
0.50	0.71	0.9000	0.50	0.71	1.2000
0.55	0.79	0.7281	0.55	0.79	0.9625
0.60	0.86	0.5375	0.60	0.86	0.7000
0.65	0.93	0.3281	0.65	0.93	0.4125
0.70	1.00	0.1000	0.70	1.00	0.1000

Table 10: Axial Velocity Data for $K = 10, 12$ with $z = 1.5$

$K = 10$			$K = 12$		
r	$\frac{r}{R}$	v	r	$\frac{r}{R}$	v
0.00	0.00	2.8225	0.00	0.00	3.4333
0.05	0.07	2.8219	0.05	0.07	3.4312
0.10	0.14	2.8000	0.10	0.14	3.4000
0.15	0.21	2.7469	0.15	0.21	3.3312
0.20	0.29	2.6625	0.20	0.29	3.2250
0.25	0.36	2.5469	0.25	0.36	3.0812
0.30	0.43	2.4000	0.30	0.43	2.9000
0.35	0.50	2.2219	0.35	0.50	2.6812
0.40	0.57	2.0125	0.40	0.57	2.4250
0.45	0.64	1.7719	0.45	0.64	2.1313
0.50	0.71	1.5000	0.50	0.71	1.8000
0.55	0.79	1.1969	0.55	0.79	1.4313
0.60	0.86	0.8625	0.60	0.86	1.0250
0.65	0.93	0.4969	0.65	0.93	0.5813
0.70	1.00	0.1000	0.70	1.00	0.1000

Figure 19 depicts the axial velocity for the pressure difference K. We use the parameters $\mu = 0.4$,$\tau_0 = 0.2$,$\delta = 0.3$,$v_s = 0.1$, and $z = 1.5$. We note that the velocities are lower than when $z = 0.8$. Similarly, the pressure difference is increasing as the axial velocity is increasing.

Figure 19: Axial velocity for K at $z = 1.5$

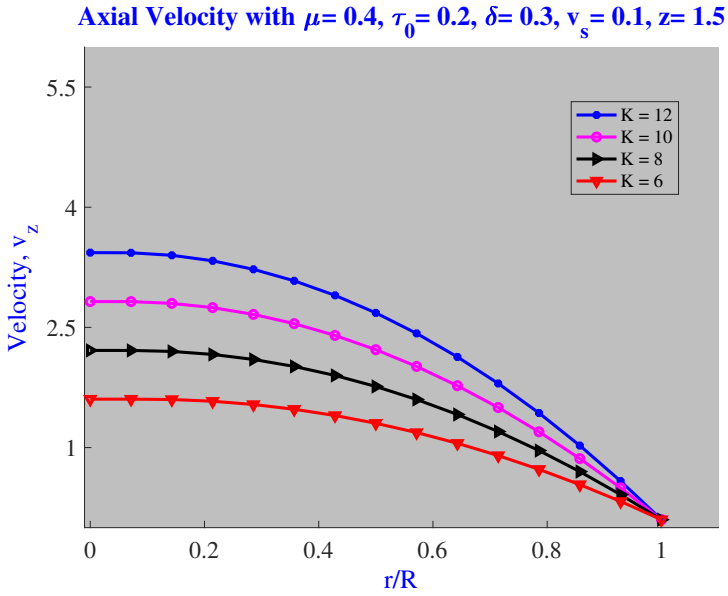

Table 11 and Table 12 present the axial velocity for various stenosis height δ. The parameters used are $\mu = 0.4$,$\tau_0 = 0.2$,$K = 8$,$v_s = 0.1$, and $z = 1.5$. There is higher axial velocity when the stenosis height is at $\delta = 0$. As the stenosis height δ is increasing, the axial velocity is decreasing.

Table 11: Axial Velocity Data for $\delta = 0, 0.1$ with $z = 1.5$

$\delta = 0$			$\delta = 0.1$		
r	$\frac{r}{R}$	v	r	$\frac{r}{R}$	v
0.00	0.00	4.6125	0.00	0.00	3.7125
0.07	0.07	4.6102	0.06	0.07	3.7115
0.14	0.14	4.5694	0.13	0.14	3.6816
0.21	0.21	4.4776	0.19	0.21	3.6105
0.29	0.29	4.3347	0.26	0.29	3.4980
0.36	0.36	4.1408	0.32	0.36	3.3441
0.43	0.43	3.8959	0.39	0.43	3.1490
0.50	0.50	3.6000	0.45	0.50	2.9125
0.57	0.57	3.2531	0.51	0.57	2.6347
0.64	0.64	2.8551	0.58	0.64	2.3156
0.71	0.71	2.4061	0.64	0.71	1.9551
0.79	0.79	1.9061	0.71	0.79	1.5533
0.86	0.86	1.3551	0.77	0.86	1.1102
0.93	0.93	0.7531	0.84	0.93	0.6258
1.00	1.00	0.1000	0.90	1.00	0.1000

Table 12: Axial Velocity Data for $\delta = 0.2, 0.3$ with $z = 1.5$

$\delta = 0.2$			$\delta = 0.3$		
r	$\frac{r}{R}$	v	r	$\frac{r}{R}$	v
0.00	0.00	2.9125	0.00	0.00	2.2125
0.06	0.07	2.9122	0.05	0.07	2.2125
0.11	0.14	2.8918	0.10	0.14	2.2000
0.17	0.21	2.8388	0.15	0.21	2.1625
0.23	0.29	2.7531	0.20	0.29	2.1000
0.29	0.36	2.6347	0.25	0.36	2.0125
0.34	0.43	2.4837	0.30	0.43	1.9000
0.40	0.50	2.3000	0.35	0.50	1.7625
0.46	0.57	2.0837	0.40	0.57	1.6000
0.51	0.64	1.8347	0.45	0.64	1.4125
0.57	0.71	1.5531	0.50	0.71	1.2000
0.63	0.79	1.2388	0.55	0.79	0.9625
0.69	0.86	0.8918	0.60	0.86	0.7000
0.74	0.93	0.5122	0.65	0.93	0.4125
0.80	1.00	0.1000	0.70	1.00	0.1000

In Figure 20, we present the axial velocity for various stenosis height δ. The parameters used are $\mu = 0.4$,$\tau_0 = 0.2$,$K = 8$,$v_s = 0.1$, and $z = 1.5$. The highest velocity is when the stenosis height is at $\delta = 0$. There is a lower velocity at a stenosis height of $\delta = 0.3$. Thus, as the stenosis height δ is increasing, the axial velocity is decreasing.

Figure 20: Axial Velocity for δ at $z = 1.5$

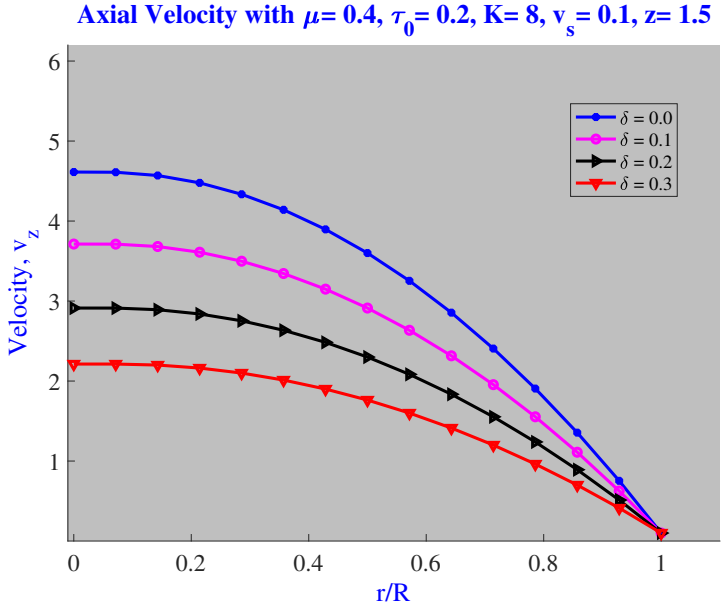

For Table 13, we present the flow rate for various δ. The parameters used are $\tau_0 = 0.2$,

$K = 8$, $\mu = 0.4$, and $v_s = 0.1$. From the data, we see that as the stenosis height δ is increasing, the flow rate Q is decreasing

Table 13: Flow Rate Data for Various δ

$\delta = 0.1$		$\delta = 0.2$		$\delta = 0.3$		$\delta = 0.5$	
z	Q	z	Q	z	Q	z	Q
0.00	7.6446	0.00	7.6446	0.00	7.6446	0.00	7.6446
0.24	7.6446	0.24	7.6446	0.24	7.6446	0.24	7.6446
0.48	7.6446	0.48	7.6446	0.48	7.6446	0.48	7.6446
0.72	7.6446	0.72	7.6446	0.72	7.6446	0.72	7.6446
1.02	7.4085	1.02	7.1779	1.02	6.9528	1.02	6.5186
1.20	5.8742	1.20	4.4328	1.20	3.2765	1.20	1.6599
1.38	5.1549	1.38	3.3334	1.38	2.0474	1.38	0.6246
1.50	5.0258	1.50	3.1500	1.50	1.8601	1.50	0.5040
1.62	5.1549	1.62	3.3334	1.62	2.0474	1.62	0.6246
1.80	5.8742	1.80	4.4328	1.80	3.2765	1.80	1.6599
1.98	7.4085	1.98	7.1779	1.98	6.9528	1.98	6.5186
2.40	7.6446	2.40	7.6446	2.40	7.6446	2.40	7.6446
2.64	7.6446	2.64	7.6446	2.64	7.6446	2.64	7.6446
2.88	7.6446	2.88	7.6446	2.88	7.6446	2.88	7.6446
3.00	7.6446	3.00	7.6446	3.00	7.6446	3.00	7.6446

Figure 21 displays the flow rate for various δ with parameters $\tau_0 = 0.2$, $K = 8$,$\mu = 0.4$,and $v_s = 0.1$. We see that the flow rate Q is highest when the stenosis height is $\delta = 0.1$ and is lowest when $\delta = 0.5$. Thus, as the stenosis height increases, the flow rate is decreasing.

Figure 21: Flow Rate for Various δ

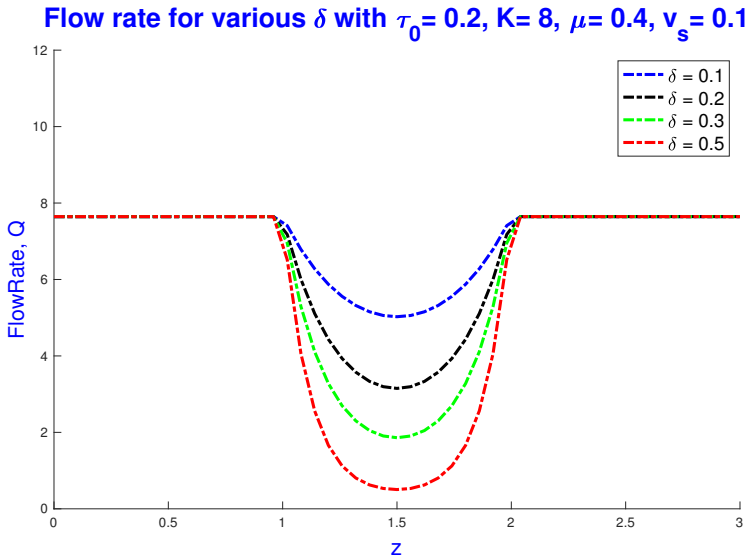

For Figure 22, we have the flow rate for various K with $\mu = 0.4$, $\tau_0 = 0.2$, $\delta = 0.3$, and $v_s = 0.1$. Here, we see that the pressure difference K has the highest flow rate Q when $K = 12$, and has the lowest flow rate when $K = 6$. Hence, as the pressure difference is increasing, the flow rate is increasing.

Figure 22: Flow Rate for Various K

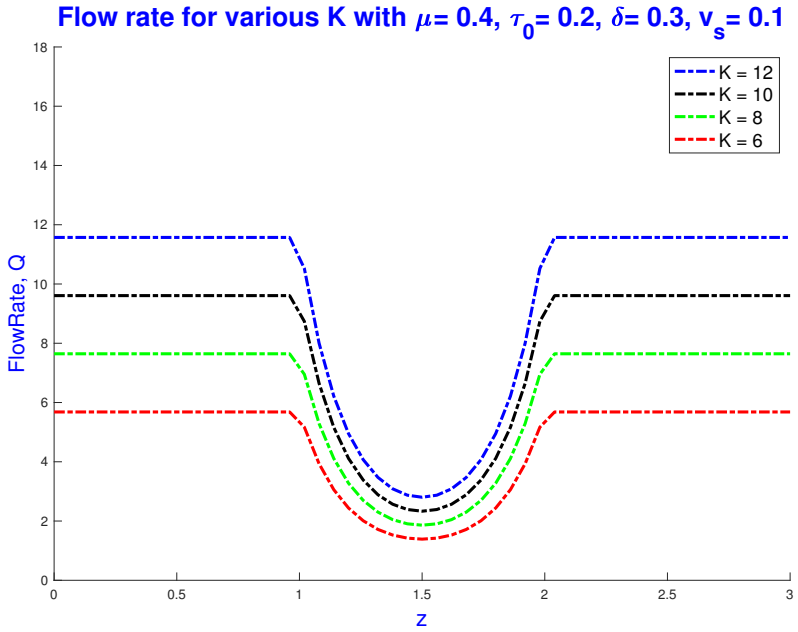

In Table 14, we present flow rate for various μ with parameters $\tau_0 = 0.2$, $K = 8$, $\delta = 0.3$, $v_s = 0.1$. We see that the flow rate values appear to be decreasing. Therefore, as the viscosity μ is increasing, the flow rate Q is decreasing.

Table 14: Flow Rate Data for Various μ

$\mu = 0.3$		$\mu = 0.4$		$\mu = 0.5$		$\mu = 0.6$	
z	Q	z	Q	z	Q	z	Q
0.00	10.0880	0.00	7.6446	0.00	6.1785	0.00	5.2011
0.18	10.0880	0.18	7.6446	0.18	6.1785	0.18	5.2011
0.54	10.0880	0.54	7.6446	0.54	6.1785	0.54	5.2011
0.72	10.0880	0.72	7.6446	0.72	6.1785	0.72	5.2011
1.02	9.1705	1.02	6.9528	1.02	5.6221	1.02	4.7350
1.20	4.3003	1.20	3.2765	1.20	2.6622	1.20	2.2527
1.38	2.6760	1.38	2.0474	1.38	1.6702	1.38	1.4188
1.50	2.4288	1.50	1.8601	1.50	1.5189	1.50	1.2914
1.62	2.6760	1.62	2.0474	1.62	1.6702	1.62	1.4188
1.80	4.3003	1.80	3.2765	1.80	2.6622	1.80	2.2527
1.98	9.1705	1.98	6.9528	1.98	5.6221	1.98	4.7350
2.34	10.0880	2.34	7.6446	2.34	6.1785	2.34	5.2011
2.52	10.0880	2.52	7.6446	2.52	6.1785	2.52	5.2011
2.70	10.0880	2.70	7.6446	2.70	6.1785	2.70	5.2011
3.00	10.0880	3.00	7.6446	3.00	6.1785	3.00	5.2011

In Figure 23, we present the flow rates for various μ with parameters $\tau_0 = 0.2$,$K = 8$,$\delta = 0.3$,$v_s = 0.1$. Here, the flow rate is higher when $\mu = 0.3$ and is lower when $\mu = 0.6$. Thus, as the viscosity increases, the flow rate is decreasing.

Figure 23: Flow Rate for Various μ

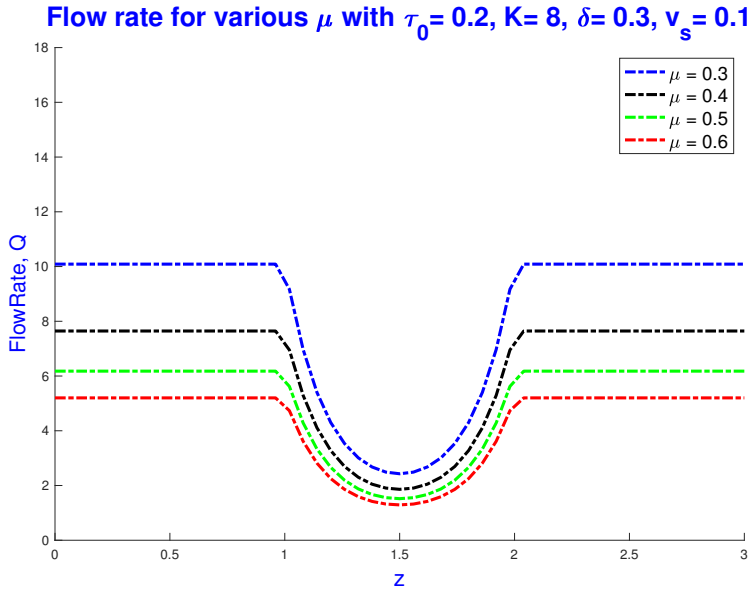

For Figure 24, we have the flow rate for various τ_0. We use parameters $\mu = 0.4$, $K = 8$,

$\delta = 0.3$, and $v_s = 0.1$. The flow rate Q is at its highest when $\tau_0 = 0.1$ and it is at its lowest when $\tau_0 = 0.7$. Therefore, as the yield stress increases, the flow rate is decreasing.

Figure 24: Flow Rate for Various τ_0

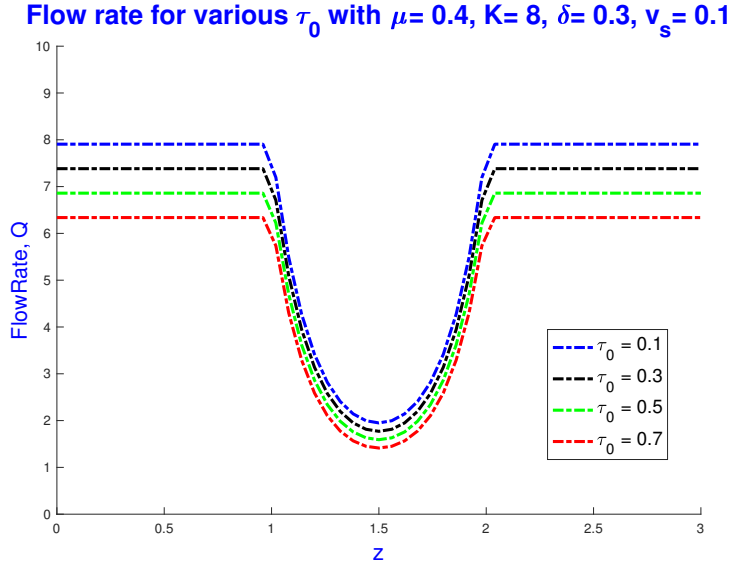

For Table 15, we have the flow rate for different v_s with parameters $\mu = 0.4$, $K = 8$,$\delta = 0.3$,and $\tau_0 = 0.2$. The flow rate values appear to increasing. Hence, as the slip velocity v_s is increasing, the flow rate Q is increasing.

Table 15: Flow Rate Data for Various v_s

$v_s = 0.0$		$v_s = 0.2$		$v_s = 0.4$		$v_s = 0.6$	
z	Q	z	Q	z	Q	z	Q
0.00	7.3304	0.00	7.9587	0.00	8.5870		9.2154
0.36	7.3304	0.36	7.9587	0.36	8.5870	0.36	9.2154
0.54	7.3304	0.54	7.9587	0.54	8.5870	0.54	9.2154
0.90	7.3304	0.90	7.9587	0.90	8.5870	0.90	9.2154
1.02	6.6532	1.02	7.2524	1.02	7.8515	1.02	8.4506
1.20	3.0714	1.20	3.4816	1.20	3.8918	1.20	4.3020
1.38	1.8857	1.38	2.2090	1.38	2.5323	1.38	2.8555
1.50	1.7062	1.50	2.0140	1.50	2.3219	1.50	2.6298
1.62	1.8857	1.62	2.2090	1.62	2.5323	1.62	2.8555
1.80	3.0714	1.80	3.4816	1.80	3.8918	1.80	4.3020
1.98	6.6532	1.98	7.2524	1.98	7.8515	1.98	8.4506
2.16	7.3304	2.16	7.9587	2.16	8.5870	2.16	9.2154
2.70	7.3304	2.70	7.9587	2.70	8.5870	2.70	9.2154
2.88	7.3304	2.88	7.9587	2.88	8.5870	2.88	9.2154
3.00	7.3304	3.00	7.9587	3.00	8.5870	3.00	9.2154

Figure 25 presents the flow rate for different v_s with parameters $\mu = 0.4$, $K = 8$,$\delta = 0.3$,and $\tau_0 = 0.2$. We see that the flow rate is highest when $v_s = 0.6$ and similarly the flow rate is lowest when $v_s = 0$. Thus, as the slip velocity increases, the flow rate increases as well.

Figure 25: Flow Rate for Various v_s

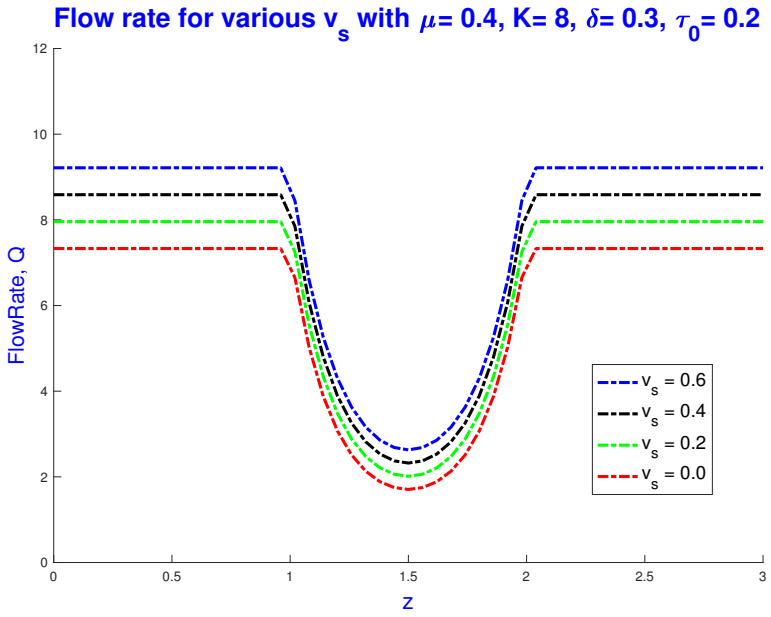

Conclusion

In this work, an analysis of blood flow through an artery in the presence of a stenosis has been carried out. Blood was treated as an incompressible, viscous and non-Newtonian (Bingham) fluid. A set of partial differential equations consisting of the equation of continuity and the momentum equation are derived first. These equations were applied to analyze the effect of the stenosis on the blood flow by computing the axial velocity and volumetric flow rate through the artery. From the computational results obtained using MATLAB, it is observed that stenosis growth has enormous impact on the axial velocity and flow rate. Increase in the stenosis height decreases the axial velocity and the flow rate. The velocity and flow rate are minimum when the stenosis height is maximum. The slip velocity has a positive effect on the axial velocity and the flow rate. It is found that the yield stress has an opposite effect on both dependent variables. Increase in pressure drop increases the axial velocity and flow rate, whereas an increase in viscosity decreases these two variables. Given these results, it is clear that the effect on stenosis on an artery is greatly influenced by stenosis height, slip velocity, pressure drop, yield stress and viscosity. It is found that the axial velocity is highest at the center of the artery or constant around the center of the artery. The axial velocity and flow rate are lowest at the peak of the stenosis. The axial velocity and flow rate display a decrease as the stenosis height increases and reaches their minimum at the peak of the stenosis. I would like to thank the committee members for their suggestions. They are incorporated is this version.

REFERENCES

[1] Chhabra, R. P. and Richardson, J.F. (2008). *Non-Newtonian Flow and Applied Rheology*, Second Edition, Butterworth-Heinemann/Elsevier.

[2] Alderman, Neil. (1997). Non-Newtonian Fluids: Guide to Classification and Characteristics.

[3] [Blood Flow in Heart] https://www.stanfordchildrens.org/content-public/topic/images/64/125864.gif.

[4] Fryar, C. D., Chen, T. C., & Li, X. (2012). Prevalence of uncontrolled risk factors for cardiovascular disease: United States, 1999-2010 (No. 103). *US Department of Health and Human Services, Centers for Disease Control and Prevention, National Center for Health Statistics*.

[5] [Normal Artery and Artery With Stenosis] https://www.123rf.com/photo_12495347_illustration-of-the-effects-of-atherosclerosis.html?vti=meebcxz8zrsu57yd6s-1-5

[6] Centers for Disease Control and Prevention. Underlying Cause of Death, 1999–2018. *CDC WONDER Online Database. Atlanta, GA: Centers for Disease Control and Prevention;* 2018.

[7] Siddiqui, S. U., & Shah, S. R. (2015). A bio-mechanical approach to study the effect of body acceleration and slip velocity through stenotic artery. *Applied Mathematics and Computation,* 261, 148-155.

[8] Singh, A., Shrivastav, R. K., & Bhatnagar, A. (2015). A numerical analysis for the effect of slip velocity and stenosis shape on non-newtonian flow of blood. *International Journal of Engineering*, 28(3), 440-446.

[9] Bunonyo, K. W., Israel-Cookey, C., & Amos, E. (2018). Modeling of blood flow through stenosed artery with heat in the presence of magnetic field. *Asian Research Journal of Mathematics,* 1-14.

[10] Misra, J. C., Patra, M. K., & Misra, S. C. (1993). A non-Newtonian fluid model for blood flow through arteries under stenotic conditions. *Journal of biomechanics*, 26(9), 1129-1141.

[11] Chakravarty, S., & Mandal, P. K. (1994). Mathematical modeling of blood flow through an overlapping arterial stenosis. *Mathematical and computer modelling,* 19(1), 59-70.

[12] Sankar, D. S., & Lee, U. (2009). Mathematical modeling of pulsatile flow of non-Newtonian fluid in stenosed arteries. *Communications in Nonlinear Science and Numerical Simulation,* 14(7), 2971-2981.

[13] Biswas, D., & Laskar, R. B. (2011). Steady flow of blood through a stenosed artery: A non-Newtonian fluid model. *Assam University Journal of Science and Technology*, 7(2), 144-153.

[14] Mathur, P., & Jain, S. (2013). Mathematical modeling of non-Newtonian blood flow through artery in the presence of stenosis. *Advances in Applied Mathematical Biosciences*, 4(1), 1-12.

[15] Mandal, P. K. (2005). An unsteady analysis of non-Newtonian blood flow through tapered arteries with a stenosis. *International Journal of Non-Linear Mechanics*, 40(1), 151-164. Chicago.

[16] Ismail, Z., Abdullah, I., Mustapha, N., & Amin, N. (2008). A power-law model of blood flow through a tapered overlapping stenosed artery. Applied Mathematics and Computation, 195(2), 669-680. Chicago.

[17] Bhatta, D. and Riahi, D. (2020). Thermal diffusivity variation effect on a hydro-thermal convective flow in a porous medium. *Journal of Porous Media*, 23(5), 497-515.

BIOGRAPHICAL SKETCH

Martin Carrillo, born June 14, 1997, grew up in Roma, TX. He graduated from Roma High school in 2015. He attended the University of Texas-Rio Grande Valley from 2015 to 2019 and received a Bachelor's of Science in Mathematics with a concentration in applied mathematics. He was awarded his Masters of Science in Mathematics with a concentration in applied mathematics in May 2021 from the University of Texas Rio Grande Valley. He was a member in the Society for Industrial and Applied Mathematics (SIAM). His personal email is martincarrillo73@yahoo.com.